

β -detected NMR of $^8\text{Li}^+$ in 1-ethyl-3-methylimidazolium acetate

Derek Fujimoto,^{1,2,*} Ryan M. L. McFadden,^{2,3} Martin H. Dehn,^{1,2} Yael Petel,³ Aris Chatzichristos,^{1,2} Lars Hemmingsen,⁴ Victoria L. Karner,^{2,3} Robert F. Kiefl,^{1,2,5} C. D. Philip Levy,⁵ Iain McKenzie,^{5,6} Carl A. Michal,³ Gerald D. Morris,⁵ Matthew R. Pearson,⁵ Daniel Szunyogh,⁴ John O. Ticknor,^{2,3} Monika Stachura,^{5,†} and W. Andrew MacFarlane^{2,3,5,‡}

¹*Department of Physics and Astronomy, University of British Columbia, Vancouver, BC V6T 1Z1, Canada*

²*Stewart Blusson Quantum Matter Institute, University of British Columbia, Vancouver, BC V6T 1Z4, Canada*

³*Department of Chemistry, University of British Columbia, Vancouver, BC V6T 1Z1, Canada*

⁴*Department of Chemistry, University of Copenhagen, 2100 København Ø, Denmark*

⁵*TRIUMF, Vancouver, BC V6T 2A3, Canada*

⁶*Department of Chemistry, Simon Fraser University, Burnaby, BC V5A 1S6, Canada*

(Dated: January 27, 2023)

We report β -detected NMR (β -NMR) spin-lattice relaxation and resonance measurements of $^8\text{Li}^+$ implanted in 1-ethyl-3-methylimidazolium acetate, an ionic liquid. The motional narrowing of the resonance line, and the local maxima in the spin-lattice relaxation rate imply a sensitivity to sub-nanosecond Li^+ solvation dynamics. From an analysis of the spin-lattice relaxation rate $1/T_1$, we extract an activation energy $E_A = 87.3(20)$ meV and Vogel-Fulcher-Tammann constant $T_{\text{VFT}} = 160.1(11)$ K, in agreement with the dynamic viscosity of the bulk solvent. Near the melting point, the lineshape is broad and intense, reflective of our sensitivity to heterogeneous dynamics near the glass transition. These findings demonstrate that ^8Li β -NMR is an effective probe of room temperature ionic liquids (RTILs).

I. INTRODUCTION

Room temperature ionic liquids (RTILs) are a fascinating class of amorphous materials with many practical applications,^{1,2} such as a lubricant in the low-pressure environments found in space-based applications.³ As in high temperature molten salts, strong Coulomb forces yield a liquid with significant structure. Pair distribution functions from scattering experiments reveal an ion arrangement of alternating charges,^{4–6} resulting in a large and strongly temperature dependent viscosity η . In contrast to simple salts, RTILs consist of large, low-symmetry molecular ions and they remain liquid at ambient temperature. Many RTILs are notoriously difficult to crystallize. Rather, they are easily supercooled, eventually freezing into a glassy state at T_g far below the thermodynamic melting point, T_m .⁷

A key feature of supercooled liquids and glasses is *dynamic heterogeneity*.^{8–10} Distinct from homogeneous liquid or crystalline phases, the local molecular dynamics (MD) of these materials exhibit fluctuations which are transient in both time and space. With highly localized probes in the form of nuclear spins, nuclear magnetic resonance (NMR) is one of the few methods with the spatial and temporal resolution to quantify this heterogeneity and reveal its characteristics.^{10,11} The degree of heterogeneity can be modelled by the “stretching” of an exponential nuclear spin-lattice relaxation (SLR), $\exp\{-(\lambda t)^\beta\}$, where $\lambda = 1/T_1$. Single exponential relaxation, corresponding to homogeneous dynamics, occurs when the stretching factor $\beta = 1$. When $\beta < 1$, the function may be decomposed according to a broad distribution of exponentials.¹² Stretched SLR may occur from a similar distribution of probe nuclei, each relaxing

exponentially with a different local rate. The breadth of this distribution is determined by β , with $\beta = 1$ corresponding to a delta function.

While stretched exponential relaxation is suggestive of dynamic heterogeneity, it does not exclude the possibility of a population which homogeneously relaxes in an intrinsically stretched manner. To this point, MD simulations of a supercooled model binary liquid have shown β to be independent of scale, at least to a few hundred atoms.¹³ Outside of this few-particle limit, this implies that the stretching is intrinsic and homogeneous. However, the NMR nuclei are each coupled to an extremely local region, far from the scale of hundreds of atoms, and are capable of identifying dynamical heterogeneity.¹¹ This sensitivity is clearly demonstrated by 4D exchange NMR, where subsets of nuclei in supercooled polyvinyl acetate were tracked by their local relaxation rate, revealing a broad distribution of relaxation times.¹⁴ Additionally, it was demonstrated that dynamical heterogeneities are a prerequisite for stretched exponential relaxation of random walkers in a random distribution of traps, a representation closely resembling our measurement in RTILs.¹⁵ A reduction of β below 1 thus represents a signature of dynamic heterogeneity.

Potential applications of the RTIL 1-ethyl-3-methylimidazolium acetate (EMIM-AC), with ions depicted in Figure 1, have motivated detailed studies of its properties, including neutron scattering measurements of its liquid structure,⁶ studies of its bulk physical properties,^{16–25} and its ability to dissolve cellulosic material.^{26,27} We use implanted-ion β -detected NMR (β -NMR) to study the development of dynamic heterogeneity and ionic mobility of implanted $^8\text{Li}^+$ in supercooled EMIM-AC.^{16,28} The β -NMR signal is due to the anisotropic β -decay of a radioisotope NMR nucleus,

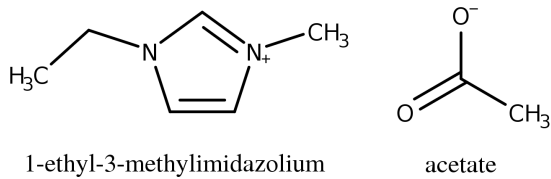


FIG. 1. Structure of the EMIM cation (*left*) and AC anion (*right*).

similar to muon spin rotation. The probe in our case is the short-lived $^8\text{Li}^+$, produced as a low-energy spin-polarized ion beam and implanted into the sample.²⁹ At any time during the measurement, the $^8\text{Li}^+$ are present in the sample at ultratrace (10^{-13} M) concentration. Implanted-ion β -NMR has been developed primarily for studying solids, particularly thin films. It is not easily amenable to liquids, since the sample must be mounted in the beamline vacuum, yet the exceptionally low vapor pressure of RTILs makes the present measurements feasible.³⁰

We have measured the strong temperature dependence of the SLR ($1/T_1$) and resonance of $^8\text{Li}^+$ in EMIM-AC. The relaxation shows a characteristic Bloembergen-Purcell-Pound (BPP) peak at 298 K, coinciding with the emergence of dynamical heterogeneity, indicated by stretched exponential relaxation. Resonance measurements clearly demonstrate motional narrowing as the RTIL is heated out of the supercooled regime. Our findings show that β -NMR could be used as a powerful technique to probe depth-resolved dynamics in *thin films* of RTILs.³¹

II. EXPERIMENT

β -NMR experiments were performed at TRIUMF's ISAC facility in Vancouver, Canada. A highly polarized 19 keV beam of $^8\text{Li}^+$ was implanted into the sample in the high-field β -NMR spectrometer with static field $B_0 = 6.55$ T.^{32,33} The incident beam had a typical flux of $\sim 10^6$ ions/s over a beam spot ~ 2 mm in diameter. Spin-polarization of the ^8Li nucleus was achieved in-flight by collinear optical pumping with circularly polarized light, yielding a polarization of $\sim 70\%$.³⁴ The $^8\text{Li}^+$ probe has nuclear spin $I = 2$, gyromagnetic ratio $\gamma = 6.3016$ MHz T $^{-1}$, nuclear electric quadrupole moment $Q = +32.6$ mb, and radioactive lifetime $\tau_\beta = 1.21$ s. The nuclear spin-polarization of ^8Li is monitored through its anisotropic β -decay, and the observed *asymmetry* of the β -decay is proportional to the average longitudinal nuclear spin-polarization.²⁹ The proportionality factor is fixed and is determined by the β -decay properties of ^8Li and the detector geometry.

Similar to other quadrupolar ($I > 1/2$) nuclei in non-magnetic materials, the strongest interaction between the

^8Li nuclear spin and its surroundings is typically the electric quadrupolar interaction, even when the time average of this interaction is zero. It is very likely that the relaxation is due primarily to fluctuations in the local electric field gradient (EFG) at the position of the ^8Li nucleus. The relaxation of a single $I = 2$ nucleus is fundamentally mono- or bi-exponential, regardless of the functional form of the EFG spectral density.³⁵

SLR measurements use a pulsed $^8\text{Li}^+$ beam. The transient decay of spin-polarization is monitored both during and following a 4 s pulse, where the polarization approaches a steady-state value during the pulse, and relaxes to ~ 0 afterwards. The effect is a pronounced kink at the end of the beam pulse, characteristic of β -NMR SLR data (Figure 2). No radio frequency (RF) magnetic field is required for the SLR measurements, as the probe nuclei are implanted in a spin state already far from thermal equilibrium. Thus, it is typically faster and easier to measure SLR than to measure the resonance spectrum; however, this type of relaxation measurement has no spectral resolution, contrary to conventional NMR, and reflects the spin relaxation of *all* the ^8Li .

Resonances were acquired by stepping a continuous wave (CW) transverse RF magnetic field slowly through the ^8Li Larmor frequency, with a continuous $^8\text{Li}^+$ beam. In the absence of spectral diffusion, the spin of any on-resonance ^8Li is rapidly nutated by the RF field, resulting in a loss in time-averaged asymmetry.

The sample consisted of a solution of 25 mM LiCl dissolved in 1-ethyl-3-methylimidazolium acetate (Sigma-Aldrich). To avoid the response being dominated by trace-level Li-trapping impurities, we introduced the stable isotope “carrier” (LiCl) at low, but macroscopic concentration (25 mM) to saturate impurity Li^+ binding sites. Additional characterization can be found in Ref. 30. The solution was kept in a dry-pumped rough vacuum for approximately 12 h prior to the measurement. A ~ 3 μL droplet was placed in a 3 mm diameter blank hole set 0.5 mm into a 1 mm thick aluminum plate. The Al plate was then bolted vertically into an ultrahigh vacuum (10^{-10} Torr) coldfinger liquid He cryostat and the temperature was varied from 220 K to 315 K. The viscosity was sufficient to prevent the liquid from flowing out of the holder during the experiment. Sample mounting involved a few minutes exposure to air, followed by pumping for 30 min in the spectrometer's load lock.

Separately, we determined the self-diffusion coefficients of the LiCl EMIM-AC solution using conventional bipolar pulsed field gradient (PFG) NMR with an in-house probe³⁶ and spectrometer³⁷ at 8.4 T and room temperature. A gradient pulse of $\delta = 3.2$ ms was applied in varying strength, g , from 50 G cm $^{-1}$ to 1200 G cm $^{-1}$. The frequency was set to either ^1H or ^7Li , and the diffusion time Δ was varied between 100 ms to 450 ms, according to the species diffusion rate. An acquisition delay of 30 ms was used in order to allow eddy currents to decay before acquisition. Diffusion coefficients were extracted by fitting the resulting Gaussian to the Stejskal-Tanner

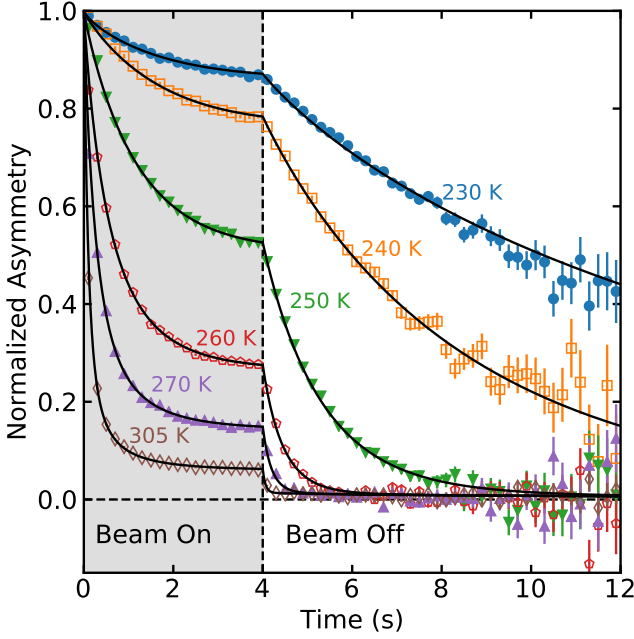


FIG. 2. The strongly temperature-dependent SLR in EMIM-AC are well described by a stretched exponential (Equation (1)) convoluted with the square beam pulse, as evidenced by $\tilde{\chi}_{\text{global}}^2 \approx 0.99$. The data have been binned by a factor of 20 for clarity. See text for analysis details.

diffusion equation.³⁸

III. RESULTS AND ANALYSIS

A. Relaxation

Typical SLR measurements are shown in Figure 2. Clearly, the relaxation shows a strong temperature dependence. At low temperatures it is slow, but its rate increases rapidly with a maximum near room temperature. Besides the rate, the *form* of the relaxation also evolves with temperature. At low temperature it is highly non-exponential, but gradually crosses-over to nearly exponential at room temperature. For a $^8\text{Li}^+$ ion implanted at time t' , the spin polarization at time $t > t'$ is well-described by a stretched exponential:

$$P(t, t') = \exp \left\{ -[\lambda(t - t')]^\beta \right\}, \quad (1)$$

where t' is integrated out as a result of convolution with the 4 s beam pulse.³⁹ A very small fraction, about 2%, of the SLR signal can be attributed to $^8\text{Li}^+$ stopping in the sample holder. While this background signal is nearly negligible, it is accounted for by $P_h(t, t') = \exp \left\{ -[\lambda_h(t - t')]^{0.5} \right\}$. The relaxation rate, λ_h , was obtained from a separate calibration run in the empty holder at 300 K and was assumed to follow the Korringa law: $\lambda_h \propto T$.

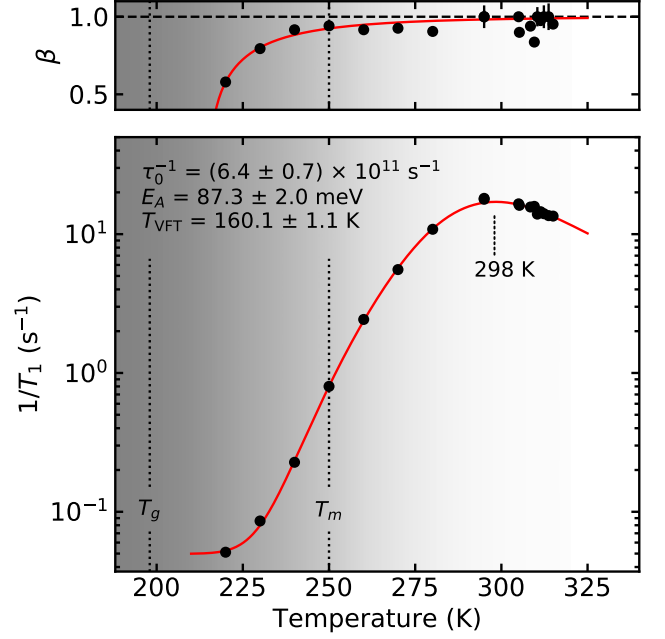


FIG. 3. Fits to the SLR, illustrated in Figure 2, reveal that both the rate ($1/T_1$) and the stretching exponent (β) are highly temperature dependent. Both show a monotonic increase until the $1/T_1$ BPP⁴² peak at 298 K, after which $\beta \approx 1$. For $1/T_1$, the line denotes a fit using Equations (2) to (4), as detailed in the text. For β , the line is a guide for the eye. The shaded region indicates the approximate temperature range of supercooling: between T_g and T_m .

The SLR time series at all T were fit simultaneously with a shared common initial asymmetry. To find the global least-squares fit, we used C++ code leveraging the MINUIT⁴⁰ minimization routines implemented within ROOT,⁴¹ accounting for the strongly time-dependent statistical uncertainties in the data. Fitting quality was excellent, with $\tilde{\chi}_{\text{global}}^2 \approx 0.99$.

As shown in Figure 3, the change in $1/T_1$ over the measured 100 K range is remarkable, varying over 3 orders of magnitude. These changes coincide with the relaxation converging to monoexponentiality with increasing temperature, as evidenced by $\beta \rightarrow 1$. The temperature dependence of $1/T_1$ is, however, not monotonic; the rate is clearly maximized at room temperature, corresponding to a BPP peak.⁴² At this temperature, the characteristic fluctuation rate of the dynamics responsible for the SLR (τ_c^{-1}) matches the probe's Larmor frequency ($\omega_0 = \gamma H_0$), i.e. $\tau_c \omega_0 \approx 1$. The SLR due to a fluctuating EFG coupled to the ^8Li , can be described by the following simple model:⁴²

$$\frac{1}{T_1} = a [J_1(\omega_0) + 4J_2(2\omega_0)] + b, \quad (2)$$

where a is a coupling constant related to the strength of the EFG, b is a phenomenological temperature-independent relaxation rate, and the J_n are the n -quantum NMR spectral density functions. The param-

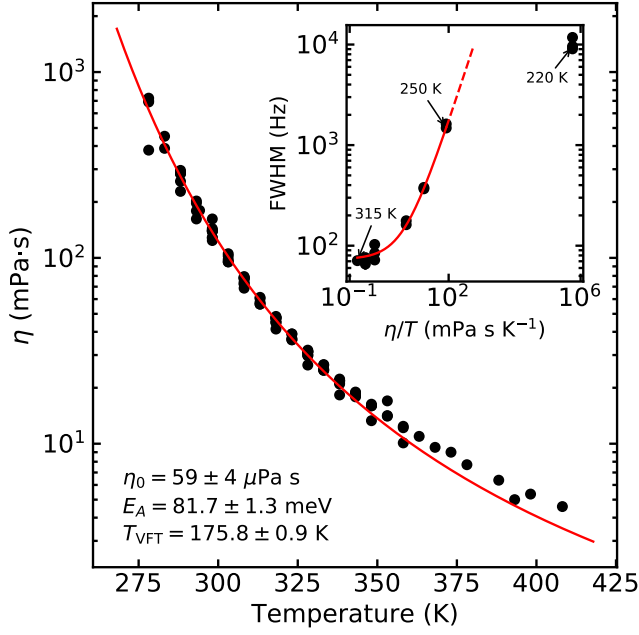


FIG. 4. The dynamic viscosity (η) compiled from the literature^{16–27} is super-Arrhenius, showing that EMIM-AC is a fragile glass former. The line is a fit to a VFT model equivalent to Equation (4), under the replacement $\tau \leftrightarrow \eta$. *Inset*: the resonance FWHM scales linearly with η/T for $T \geq 250$ K, as expected from a Stokes-Einstein description. Inset line is a linear fit.

ters a and b are $1.550(2) \times 10^9 \text{ s}^{-2}$ and $4.98(2) \times 10^{-2} \text{ s}^{-1}$ respectively. If the local dynamics relax exponentially, the spectral density has the Debye (Lorentzian) form:

$$J_n(n\omega) = \frac{2\tau_c}{1 + (n\omega\tau_c)^2}, \quad (3)$$

where τ_c is the correlation time.

Local fluctuations may be related to other macroscopic properties of the liquid such as the viscosity. Using values from the literature,^{16–27} Figure 4 shows that the viscosity of EMIM-AC is non-Arrhenius and can be described with the phenomenological Vogel-Fulcher-Tammann (VFT) model. We assume our local correlation time τ_c follows the same:

$$\tau_c = \tau_0 \exp \left[\frac{E_A}{k_B (T - T_{\text{VFT}})} \right], \quad (4)$$

where τ_0 is a prefactor, E_A is the activation energy, k_B is the Boltzmann constant, T is the absolute temperature, and T_{VFT} is a constant. Together, Equations (2) to (4) encapsulate the temperature and frequency dependence of the ^8Li $1/T_1$ in the supercooled ionic liquid. A fit of the data to this model is shown in Figure 3. The correlation times from 220 K to 315 K are on the order of nanoseconds. The choice of Equation (3) assumes that the $\beta < 1$ stretching arises from a population of exponential relaxing environments with a broad distribution of

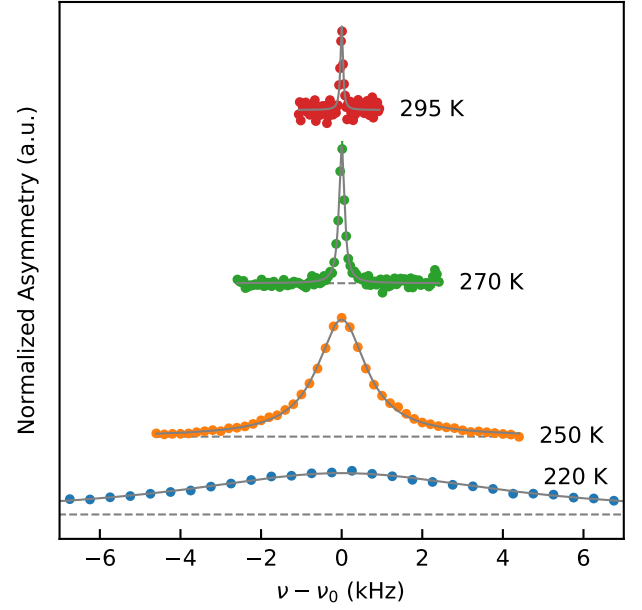


FIG. 5. As the temperature is raised, the ^8Li resonance in EMIM-AC narrows and increases in height, with a peak in the latter near 260 K (see Figure 6). The vertical scale is the same for all spectra, which have been offset for clarity. Solid lines denote Lorentzian fits and ν_0 is the Larmor frequency. Spectra are inverted for consistency with conventional NMR.

relaxation times. As mentioned, this assumption is likely good for the ^8Li β -NMR probe; especially since the basic local relaxation of ^8Li due to quadrupolar coupling is not intrinsically stretched, independent of the form of the dynamical fluctuation spectrum.³⁵ Under this construction, the departure from $\beta = 1$ in the supercooled regime implies the emergence of dynamical heterogeneity.

B. Resonance

Typical ^8Li resonances are shown in Figure 5. Similar to the SLR, they show a strong temperature dependence. At low T , the resonance is broad with a typical solid-state linewidth on the order of 10 kHz. The absence of resolved quadrupolar splitting indicates that the average EFG is zero; the width likely represents an inhomogeneous distribution of static EFGs giving a broad “powder pattern” lineshape convoluted with the CW NMR excitation, a Lorentzian of width γH_1 , where $H_1 \approx 0.1$ G. This inhomogeneous quadrupolar broadening is qualitatively consistent with the heterogeneity in the dynamics implied by the stretched exponential relaxation.

The resonances are well-described by a simple Lorentzian. The baseline (time-integrated) asymmetry is also strongly temperature dependent due to the temperature dependence of $1/T_1$. The shift of the resonance relative to a single crystal of MgO (our conventional fre-

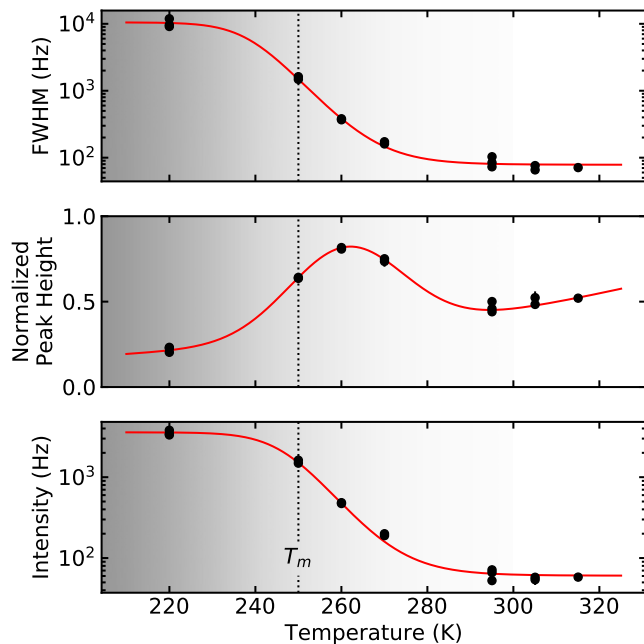


FIG. 6. As the temperature is raised past the melting point, molecular motion of the solvent averages the ^8Li resonance to a narrow Lorentzian. The mirrored drop in intensity (area of the normalized spectra), and the peak in the height near 260 K suggests that the line is inhomogeneously broadened at low temperature, and that slow spectral dynamics occur on the scale of the integration time at each frequency (1 s). Lines are to guide the eye.

quency standard) is about -9 ppm, but a slow drift of the magnetic field prevents an accurate determination or a reliable measurement of any slight T dependence. The other fit parameters extracted from this analysis are shown in Figure 6.

As anticipated from the most striking features in Figure 5, the linewidth and peak height evolve considerably with temperature. Note that the peak height in Figure 6 is measured from the baseline, and is normalized to be in units of the baseline value. Both of these measures account for changes in the SLR. Reduction in the linewidth by several orders of magnitude is compatible with motional narrowing, where rapid molecular motion averages out static inhomogeneous broadening. Saturation of the narrowing by room temperature with onset far below the $1/T_1$ maximum is consistent with the BPP interpretation of the peak.⁴²

IV. DISCUSSION

Through a strong Coulomb interaction, RTILs are known to contain a significant amount of structure. One might expect pairing of anions and cations, but calculations based on a simplified ion interaction model suggest that such pairs are short-lived.⁴³ Dielectric relax-

ation confirms this, placing a 100 ps upper bound to their lifetime, rendering them a poor description of the average ionic structure.⁴⁴ Rather, the arrangement can be described as two interpenetrating ionic networks. As revealed by neutron scattering,⁴⁻⁶ each network forms cages about the other that are highly anisotropic due to the tendency for EMIM rings to stack.⁶ In fragile glass formers, such as EMIM-AC, MD simulations indicate that the motion of the caged ion and the center of mass motion of the cage are correlated.⁴⁵ Presumably, in our case, the small $^8\text{Li}^+$ cation is coordinated by several acetates and a similar correlation will exist for the $^8\text{Li}^+$ in the absence of independent long-range diffusion.

Naturally, the motion of the surrounding ionic solvent cage will cause the EFG to fluctuate, and a strong temperature dependence is reasonable since these same fluctuations have a role in determining the strongly temperature dependent viscosity $\eta(T)$ shown in Figure 4. While a direct relation between the specific motions sensed by ^8Li and the bulk η is complex and unclear,⁴⁶ one may anticipate a consistency between their kinetics should a single mechanism govern both. The similarity of both E_A and T_{VFT} with those found from the viscosity of the pure EMIM-AC suggests that this is the case and provides further justification for the choice of Equation (4).

The inset of Figure 4 shows that motional narrowing causes the resonance linewidths to scale as η/T in the liquid state above T_g , a situation also observed in DEME-TFSA with solute ^7Li NMR.⁴⁷ That this relationship holds is surprising. The NMR signal is due to the dynamics of a population of implanted local probes, for which solvent self-diffusion and probe tracer-diffusion are not differentiated, whereas the viscosity is a bulk property. If Li is diffusing, this implies that the diffusion is controlled by the solvent dynamics. In the limiting case, interstitial diffusion can be fast, yet the viscosity infinite, such as in solid state ionic conductors where the decoupling of diffusion and the host viscosity is self-evident. Many RTILs violate the Stokes-Einstein relation that linearly relates self-diffusivity D to T/η , and its violation at low T in the inset of Figure 4 shows that ionic diffusion in supercooled RTILs may contain some of the character expected from a solid. At 295 K however, our PFG NMR in EMIM-AC with 30 mM LiCl shows that the ^7Li diffusion is not significantly larger than the solvent ($D_{\text{Li}} = 3.46(11) \times 10^{-10} \text{ m}^2\text{s}^{-1}$ vs $D_{\text{H}} = 3.61(7) \times 10^{-10} \text{ m}^2\text{s}^{-1}$), demonstrating that we are sensitive to the mobility of the solvent cage.

Relatively little is known about Li^+ as a solute in EMIM-AC. Much more is known in other imidazolium-based RTILs, which have been explored as electrolytes for Li batteries.^{47,48} Their properties should be qualitatively comparable, but the details certainly differ as both size and shape play a role in the ion diffusivity.⁴⁹ Shown to compare favorably with implanted-ion β -NMR,³⁰ conventional NMR can provide a comparison to some closely related RTILs: EMIM-TFSA and EMIM-FSA. In both cases the diffusion of ^7Li was similar to that of the solvent

ions.⁵⁰ Differences in the tracer diffusion are reflected in the activation barrier for ^7Li hopping: 222(6) meV and 187(2) meV respectively.⁵⁰ This correlates well with anion molecular weight, 280 g mol $^{-1}$ and 180 g mol $^{-1}$, and with the barrier we report for ^8Li : 87.3(20) meV for acetate of 59 g mol $^{-1}$. This further emphasizes the probe sensitivity to the solvent dynamics.

The motional narrowing, immediately apparent in Figure 6, is analogous to conventional NMR, but the use of CW RF modifies the detailed description significantly. While the details are beyond the scope of this work, and will be clarified at a later date, we now give a qualitative description. In the slow fluctuation limit, the line is broadened relative to the static limit at $T = 0$ due to slow spectral dynamics occurring over the second-long integration time at each RF frequency. Both the peak height and the intensity (area of the normalized curve) are increased through the double counting of spins at multiple RF frequencies. In the fast fluctuation limit, the time spent with a given local environment is small and the RF is relatively ineffective at nutating the spins. Unlike the slow fluctuation limit, transverse coherence is now needed to destroy polarization. Coherence is maintained only in a small range about the Larmor frequency, narrowing as the fluctuation rate increases. The intensity (area) is also reduced from the preservation of off-resonance polarization, but the peak height is unaffected. The local maximum in the peak height is explicable from the small non-relaxing background contribution. SLR reduces the polarization of the sample signal when T_1 is much smaller than the ^8Li lifetime. This shifts the baseline, which acts as both reference and normalization for the peak height. The resulting reduction in the fraction of destroyed polarization competing with the increase from motional narrowing produces the local maximum in Figure 6.

The development of dynamic heterogeneity at the nanosecond timescale (ω_0^{-1}) is demonstrated by the stretched exponential SLR, as shown in Figure 3. Concurrently, the line broadening shows that this heterogeneity reaches down to the static timescale. There are no definitive measurements of the melting point of EMIM-AC, since it has not yet been crystallized, but T_m is no larger than 250 K.⁵¹ In contrast, a calorimetric glass transition has been observed at about $\sim 198\text{ K}$.⁵² Thus, the dynamic inhomogeneity develops in a range of T that corresponds well to the region of supercooling, indicated by the shaded region of Figure 3.

Based on the non-Arrhenius behaviour of $\eta(T)$ demonstrated in Figure 4, EMIM-AC is a reasonably fragile glass former, comparable to toluene which has been studied in some detail using conventional deuterium NMR,^{53,54} providing us with a useful point of comparison to a nonionic liquid. Like ^8Li , ^2H should exhibit primarily quadrupolar relaxation. Toluene is supercooled between its melting point 178 K and glass transition $\sim 117\text{ K}$, though it shows stretched exponential relaxation only below about $1.1 T_g$, considerably deeper into the supercooled regime than in our case, with an onset near

$1.25 T_g$, likely due to the stronger tendency to order in the ionic liquid.

The closest analogue to our experiment in EMIM-AC is, perhaps, an early (neutron activated) ^8Li β -NMR study in $\text{LiCl} \cdot 7\text{D}_2\text{O}$. There, the observed temperature dependence of the SLR is qualitatively similarly understood (see Figure 9 of Ref. 55): at low temperatures, the relaxation is nearly temperature independent, followed by a rapid increase above the glass transition, leading eventually to the BPP peak at higher temperatures. This behaviour was interpreted as the onset of molecular motion above $\sim 80\text{ K}$, whose characteristic correlation times reflect the diffusion and orientation fluctuations in D_2O . This is consistent with the picture outlined here, although in our more limited temperature range the relaxation can be ascribed to a single dynamical process.

At present, there are few examples of ^8Li β -NMR in organic materials, as this application is in its infancy. Nevertheless, several trends from these early investigations have emerged, which serve as an important point of comparison for the current results. From an initial survey on organic polymers,⁵⁶ it was remarked that resonances were generally broad and unshifted, with little or no temperature dependence. In contrast, the SLR was typically fast and independent of the proton density, implying a quadrupolar mechanism caused by the MD of the host atoms. These dynamics turned out to be strongly depth dependent, increasing on approach to a free surface⁵⁷ or buried interface.⁵⁸ In addition to dynamics of the polymer backbone, certain structures admitted Li^+ diffusion,⁵⁹ whose mobility was found to depend on the ionicity of the anion of the dissolved Li salt.⁶⁰ A few small molecular glasses have also been investigated, where the relaxation is similarly fast.⁶¹

Common to all of these studies is the non-exponential decay of the ^8Li spin-polarization, which is well described by a stretched exponential. In these disordered materials, the “stretched” behaviour is compatible with the interpretation of a distribution of local environments, leading to an inhomogeneous SLR. In the high-temperature limit, the dynamics appear to homogenize, although this limit is inaccessible in previously studied materials. EMIM-AC is an important first example where the liquid state is attainable to the degree where we recover simple exponential SLR, accompanied by motional narrowing and a BPP peak.

V. CONCLUSION

We report the first measurements of ^8Li β -NMR in a 1-ethyl-3-methylimidazolium acetate ionic liquid. Our results demonstrate that the quadrupolar interaction does not hinder our ability to follow the β -NMR signal through both the liquid and glassy state. We observed clear motional narrowing as the temperature is raised, accompanied by enhanced spin-lattice relaxation, whose rate is maximized at room temperature. From an analysis of

the temperature dependent SLR rate, we extract an activation energy and VFT constant for the solvation dynamics which are in surprisingly good agreement with the dynamic viscosity of the bulk EMIM-AC. At low temperatures near the solvent melting point, the resonance is broad and intense, reflective of our sensitivity to slow heterogeneous dynamics near the glass transition. These findings suggest that ^8Li β -NMR is a good probe of both solvation dynamics and their heterogeneity. The depth resolution of ion-implanted β -NMR may provide a unique means of studying nanoscale phenomena in ionic liquids, such as ion behaviour at the liquid-vacuum interface or the diffusivity dependence on film thickness.⁶²

ACKNOWLEDGMENTS

The authors thank R. Abasalti, D. J. Arseneau, S. Daviel, B. Hitti, and D. Vyas for their excellent technical support. This work was supported by NSERC Discovery grants to R.F.K. and W.A.M. R.M.L.M. and A.C. acknowledge the support of their NSERC CREATE IsoSiM Fellowships. D.F. and V.L.K. acknowledge the support of their SBQMI QuEST Fellowships.

* fujimoto@phas.ubc.ca

† mstachura@triumf.ca

‡ wam@chem.ubc.ca

- ¹ Robert Hayes, Gregory G. Warr, and Rob Atkin, "Structure and nanostructure in ionic liquids," *Chem. Rev.* **115**, 6357–6426 (2015).
- ² Douglas R. MacFarlane, Naoki Tachikawa, Maria Forsyth, Jennifer M. Pringle, Patrick C. Howlett, Gloria D. Elliott, James H. Davis, Masayoshi Watanabe, Patrice Simon, and C. Austen Angell, "Energy applications of ionic liquids," *Energ. Environ. Sci.* **7**, 232–250 (2014).
- ³ Kenneth W. Street Jr., Wilfredo Morales, Victor R. Koch, Daniel J. Valco, Ryan M. Richard, and Nicole Hanks, "Evaluation of vapor pressure and ultra-high vacuum tribological properties of ionic liquids," *Tribol. T.* **54**, 911–919 (2011).
- ⁴ M.P. Tosi, D.L. Price, and M.-L. Saboungi, "Ordering in metal halide melts," *Annu. Rev. Phys. Chem.* **44**, 173–211 (1993).
- ⁵ Thomas Murphy, Rob Atkin, and Gregory G. Warr, "Scattering from ionic liquids," *Curr. Opin. Colloid. In.* **20**, 282–292 (2015).
- ⁶ D. T. Bowron, C. D'Agostino, L. F. Gladden, C. Hardacre, J. D. Holbrey, M. C. Lagunas, J. McGregor, M. D. Mantle, C. L. Mullan, and T. G. A. Youngs, "Structure and dynamics of 1-ethyl-3-methylimidazolium acetate via molecular dynamics and neutron diffraction," *J. Phys. Chem. B.* **114**, 7760–7768 (2010).
- ⁷ Anja-Verena Mudring, "Solidification of ionic liquids: Theory and techniques," *Aust. J. Chem.* **63**, 544–564 (2010).
- ⁸ M. D. Ediger and Peter Harrowell, "Perspective: Supercooled liquids and glasses," *J. Chem. Phys.* **137**, 080901 (2012).
- ⁹ Edward W. Castner and James F. Wishart, "Spotlight on ionic liquids," *J. Chem. Phys.* **132**, 120901 (2010).
- ¹⁰ Hans Sillescu, "Heterogeneity at the glass transition: a review," *J. Non-Cryst. Solids.* **243**, 81–108 (1999).
- ¹¹ J.I Kaplan and A.N Garroway, "Homogeneous and inhomogeneous distributions of correlation times. Lineshapes for chemical exchange," *J. Magn. Reson.* **49**, 464–475 (1982).
- ¹² C. P. Lindsey and G. D. Patterson, "Detailed comparison of the Williams-Watts and Cole-Davidson functions," *J. Chem. Phys.* **73**, 3348–1484 (1980).
- ¹³ Baoshuang Shang, Jörg Rottler, Pengfei Guan, and Jean-Louis Barrat, "Local versus Global Stretched Mechanical

Response in a Supercooled Liquid near the Glass Transition," *Phys. Rev. Lett.* **122**, 105501 (2019).

- ¹⁴ K. Schmidt-Rohr and H. W. Spiess, "Nature of nonexponential loss of correlation above the glass transition investigated by multidimensional NMR," *Phys. Rev. Lett.* **66**, 3020–3023 (1991).
- ¹⁵ S. I. Simdyankin and Normand Mousseau, "Relationship between dynamical heterogeneities and stretched exponential relaxation," *Phys. Rev. E.* **68**, 041110 (2003).
- ¹⁶ Pierre Bonhôte, Ana-Paula Dias, Nicholas Papageorgiou, Kuppaswamy Kalyanasundaram, and Michael Grätzel, "Hydrophobic, highly conductive ambient-temperature molten salts," *Inorg. Chem.* **35**, 1168–1178 (1996).
- ¹⁷ Sebastian Fendt, Sasisanker Padmanabhan, Harvey W. Blanch, and John M. Prausnitz, "Viscosities of acetate or chloride-based ionic liquids and some of their mixtures with water or other common solvents," *J. Chem. Eng. Data.* **56**, 31–34 (2011).
- ¹⁸ Andre Pinkert, Keng L. Ang, Kenneth N. Marsh, and Shusheng Pang, "Density, viscosity and electrical conductivity of protic alkanolammonium ionic liquids," *Phys. Chem. Chem. Phys.* **13**, 5136–5143 (2011).
- ¹⁹ Ana B. Pereiro, Joao M. M. Araujo, Filipe S. Oliveira, Carlos E. S. Bernardes, Jose M. S. S. Esperanca, Jose N. Canongia Lopes, Isabel M. Marrucho, and Luis P. N. Rebelo, "Inorganic salts in purely ionic liquid media: the development of high ionicity ionic liquids (HIILs)," *Chem. Commun.* **48**, 3656–3658 (2012).
- ²⁰ María C. Castro, Alberto Arce, Ana Soto, and Héctor Rodríguez, "Thermophysical characterization of the mixtures of the ionic liquid 1-ethyl-3-methylimidazolium acetate with 1-propanol or 2-propanol," *J. Chem. Eng. Data.* **61**, 2299–2310 (2016).
- ²¹ N. P. Evlampieva, J. Vitz, U. S. Schubert, and E. I. Rymtsev, "Molecular solutions of cellulose in mixtures of ionic liquids with pyridine," *Russ. J. Appl. Chem.* **82**, 666–672 (2009).
- ²² Qingguo Zhang, Siyi Cai, Wenbo Zhang, Yalin Lan, and Xinyuan Zhang, "Density, viscosity, conductivity, refractive index and interaction study of binary mixtures of the ionic liquid 1-ethyl-3-methylimidazolium acetate with methyldiethanolamine," *J. Mol. Liq.* **233**, 471–478 (2017).
- ²³ Andreas Nazet, Sophia Sokolov, Thomas Sonnleitner, Takashi Makino, Mitsuhiro Kanakubo, and Richard Buchner, "Densities, viscosities, and conduc-

- tivities of the imidazolium ionic liquids [Emim][Ac], [Emim][FAP], [Bmim][BETI], [Bmim][FSI], [Hmim][TFSI], and [Omim][TFSI]," *J. Chem. Eng. Data*. **60**, 2400–2411 (2015).
- 24 J. M. M. Araújo, A. B. Pereiro, F. Alves, I. M. Marrucho, and L. P. N. Rebelo, "Nucleic acid bases in 1-alkyl-3-methylimidazolium acetate ionic liquids: A thermophysical and ionic conductivity analysis," *J. Chem. Thermodyn.* **57**, 1–8 (2013).
 - 25 E. Quijada-Maldonado, S. van der Boogaart, J. H. Liijbers, G. W. Meindersma, and A. B. de Haan, "Experimental densities, dynamic viscosities and surface tensions of the ionic liquids series 1-ethyl-3-methylimidazolium acetate and dicyanamide and their binary and ternary mixtures with water and ethanol at $T = (298.15 \text{ to } 343.15 \text{ K})$," *J. Chem. Thermodyn.* **51**, 51–58 (2012).
 - 26 Mara G. Freire, Ana Rita R. Teles, Marisa A. A. Rocha, Bernd Schröder, Catarina M. S. S. Neves, Pedro J. Carvalho, Dmitry V. Evtuguin, Luís M. N. B. F. Santos, and João A. P. Coutinho, "Thermophysical characterization of ionic liquids able to dissolve biomass," *J. Chem. Eng. Data*. **56**, 4813–4822 (2011).
 - 27 María C. Castro, Héctor Rodríguez, Alberto Arce, and Ana Soto, "Mixtures of ethanol and the ionic liquid 1-ethyl-3-methylimidazolium acetate for the fractionated solubility of biopolymers of lignocellulosic biomass," *Ind. Eng. Chem. Res.* **53**, 11850–11861 (2014).
 - 28 John S. Wilkes and Michael J. Zaworotko, "Air and water stable 1-ethyl-3-methylimidazolium based ionic liquids," *J. Chem. Soc. Chem. Commun.*, 965–967 (1992).
 - 29 W. A. MacFarlane, "Implanted-ion β NMR: A new probe for nanoscience," *Solid State Nucl. Magn. Reson.* **68–69**, 1–12 (2015).
 - 30 Daniel Szunyogh, Ryan M. L. McFadden, Victoria L. Karner, Aris Chatzichristos, Thomas Day Goodacre, Martin H. Dehn, Lia Formenti, Derek Fujimoto, Alexander Gottberg, Evan Kallenberg, Ildikó Kálomista, Robert F. Kiefl, Flemming H. Larsen, Jens Lassen, C. D. Philip Levy, Ruohong Li, W. Andrew MacFarlane, Iain McKenzie, Gerald D. Morris, Stavroula Pallada, Matthew R. Pearson, Stephan P. A. Sauer, Paul Schaffer, Peter W. Thulstrup, Lars Hemmingsen, and Monika Stachura, "Direct observation of Mg^{2+} complexes in ionic liquid solutions by ^{31}Mg β -NMR spectroscopy," *Dalton Trans.* **47**, 14431–14435 (2018).
 - 31 Jun Nishida, John P. Breen, Boning Wu, and Michael D. Fayer, "Extraordinary slowing of structural dynamics in thin films of a room temperature ionic liquid," *ACS Cent. Sci.* **4**, 1065–1073 (2018).
 - 32 Gerald D. Morris, " β -NMR," *Hyperfine. Interact.* **225**, 173–182 (2014).
 - 33 G. D. Morris, W. A. MacFarlane, K. H. Chow, Z. Salman, D. J. Arseneau, S. Daviel, A. Hatakeyama, S. R. Kreitzman, C. D. P. Levy, R. Poutissou, R. H. Heffner, J. E. Elenewski, L. H. Greene, and R. F. Kiefl, "Depth-controlled β -NMR of ^7Li in a thin silver film," *Phys. Rev. Lett.* **93**, 157601 (2004).
 - 34 C. D. P. Levy, R. Baartman, K. Jayamanna, R. Kiefl, T. Kuo, M. Olivo, G. W. Wight, D. Yuan, and A. N. Zelenski, "A polarized beams project at ISAC," *Nucl. Phys. A*. **701**, 253–258 (2002).
 - 35 K. D. Becker, "Nuclear Magnetic Relaxation Induced by the Dynamics of Lattice Defects in Solids ($I = 3/2, I = 2$, and $I = 5/2$)," *Z. Naturforsch.* **37a**, 697–705 (1982).
 - 36 Alison L. Michan, *Nuclear Magnetic Resonance Characterization of Solid Polymer Electrolyte Materials*, Master's thesis, The University of British Columbia (2012).
 - 37 Carl A. Michal, Kesten Broughton, and Elsa Hansen, "A high performance digital receiver for home-built nuclear magnetic resonance spectrometers," *Rev. Sci. Instrum.* **73**, 453–458 (2002).
 - 38 Edward O. Stejskal and John E. Tanner, "Spin Diffusion Measurements: Spin Echoes in the Presence of a Time-Dependent Field Gradient," *J. Chem. Phys.* **42**, 288–292 (1965).
 - 39 W. A. MacFarlane, Q. Song, N. J. C. Ingle, K. H. Chow, M. Egilmez, I. Fan, M. D. Hossain, R. F. Kiefl, C. D. P. Levy, G. D. Morris, T. J. Parolin, M. R. Pearson, H. Saadaoui, Z. Salman, and D. Wang, " β -detected NMR spin relaxation in a thin film heterostructure of ferromagnetic EuO ," *Phys. Rev. B*. **92**, 064409 (2015).
 - 40 F. James and M. Roos, "Minuit — a system for function minimization and analysis of the parameter errors and correlations," *Comput. Phys. Commun.* **10**, 343–367 (1975).
 - 41 Rene Brun and Fons Rademakers, "Root — an object oriented data analysis framework," *Nucl. Instrum. Methods Phys. Res. A* **389**, 81–86 (1997).
 - 42 N. Bloembergen, E. M. Purcell, and R. V. Pound, "Relaxation effects in nuclear magnetic resonance absorption," *Phys. Rev.* **73**, 679–712 (1948).
 - 43 Alpha A. Lee, Dominic Vella, Susan Perkin, and Alain Goriely, "Are room-temperature ionic liquids dilute electrolytes?" *J. Phys. Chem. Lett.* **6**, 159–163 (2015), pMID: 26263105.
 - 44 Corinne Daguene, Paul J. Dyson, Ingo Krossing, Alla Oleinikova, John Slattery, Chihiro Wakai, and Hermann Weingärtner, "Dielectric response of imidazolium-based room-temperature ionic liquids," *J. Phys. Chem. B*. **110**, 12682–12688 (2006), pMID: 16800602, <https://doi.org/10.1021/jp0604903>.
 - 45 Junko Habasaki and K. L. Ngai, "Rigidity and soft percolation in the glass transition of an atomistic model of ionic liquid, 1-ethyl-3-methyl imidazolium nitrate, from molecular dynamics simulations—existence of infinite overlapping networks in a fragile ionic liquid," *J. Chem. Phys.* **142**, 164501 (2015).
 - 46 J. W. Akitt, "The alkali and alkaline earth metals," in *Multinuclear NMR*, edited by Joan Mason (Springer, Boston, MA, 1987) Chap. 7, pp. 189–220.
 - 47 Atsushi Shirai and Yasuhisa Ikeda, " ^7Li NMR studies on complexation reactions of lithium ion with cryptand c211 in ionic liquids: Comparison with corresponding reactions in nonaqueous solvents," *Inorg. Chem.* **50**, 1619–1627 (2011).
 - 48 Béatrice Garcia, Serge Lavallée, Gérald Perron, Christophe Michot, and Michel Armand, "Room temperature molten salts as lithium battery electrolyte," *Electrochim. Acta*. **49**, 4583–4588 (2004).
 - 49 Hiroyuki Tokuda, Kikuko Hayamizu, Kunikazu Ishii, Md. Abu Bin Hasan Susan, and Masayoshi Watanabe, "Physicochemical properties and structures of room temperature ionic liquids. 2. variation of alkyl chain length in imidazolium cation," *J. Phys. Chem. B*. **109**, 6103–6110 (2005).
 - 50 Kikuko Hayamizu, Seiji Tsuzuki, Shiro Seki, and Yasuhiro Umebayashi, "Nuclear magnetic resonance studies on the rotational and translational motions of ionic liquids composed of 1-ethyl-3-methylimidazolium cation and bis(trifluoromethanesulfonyl)amide and

- bis(fluorosulfonyl)amide anions and their binary systems including lithium salts,” *J. Chem. Phys.* **135**, 084505 (2011).
- ⁵¹ Ning Sun, Mustafizur Rahman, Ying Qin, Mirela L. Maxim, Héctor Rodríguez, and Robin D. Rogers, “Complete dissolution and partial delignification of wood in the ionic liquid 1-ethyl-3-methylimidazolium acetate,” *Green. Chem.* **11**, 646–655 (2009).
 - ⁵² Wei Guan, Xiao-Xue Ma, Long Li, Jing Tong, Da-Wei Fang, and Jia-Zhen Yang, “Ionic parachor and its application in acetic acid ionic liquid homologue 1-alkyl-3-methylimidazolium acetate [C_nmim][OAc] (n = 2,3,4,5,6),” *J. Phys. Chem. B.* **115**, 12915–12920 (2011), pMID: 21978307, <https://doi.org/10.1021/jp207882t>.
 - ⁵³ G. Hinze and H. Sillescu, “²H nuclear magnetic resonance study of supercooled toluene: Slow and fast processes above and below the glass transition,” *J. Chem. Phys.* **104**, 314–319 (1996).
 - ⁵⁴ Roland Böhmer, Gerald Hinze, Thomas Jörg, Fei Qi, and Hans Sillescu, “Dynamical heterogeneity in α - and β -relaxations of glass forming liquids as seen by deutron NMR,” *J. Phys-Condens. Mat.* **12**, A383 (2000).
 - ⁵⁵ P. Heitjans, W. Faber, and A. Schirmer, “ β -NMR studies of spin-lattice relaxation in glassy and layer-crystalline compounds,” *J. Non-Cryst. Solids.* **131–133**, 1053–1062 (1991).
 - ⁵⁶ F. H. McGee, I. McKenzie, T. Buck, C. R. Daley, J. A. Forrest, M. Harada, R F Kiefl, C. D. P. Levy, G. D. Morris, M. R. Pearson, J. Sugiyama, D. Wang, and W. A. MacFarlane, “A brief survey of β -detected NMR of implanted ⁸Li⁺ in organic polymers,” *J. Phys. Conf. Ser.* **551**, 012039 (2014).
 - ⁵⁷ Iain McKenzie, Chad R. Daley, Robert F. Kiefl, C. D. Philip Levy, W. Andrew MacFarlane, Gerald D. Morris, Matthew R. Pearson, Dong Wang, and James A. Forrest, “Enhanced high-frequency molecular dynamics in the near-surface region of polystyrene thin films observed with β -NMR,” *Soft. Matter.* **11**, 1755–1761 (2015).
 - ⁵⁸ Iain McKenzie, Yu Chai, David L. Cortie, James A. Forrest, Derek Fujimoto, Victoria L. Karner, Robert F. Kiefl, C. D. Philip Levy, W. Andrew MacFarlane, Ryan M. L. McFadden, Gerald D. Morris, Matthew R. Pearson, and Shipai Zhu, “Direct measurements of the temperature, depth and processing dependence of phenyl ring dynamics in polystyrene thin films by β -detected NMR,” *Soft. Matter.* **14**, 7324–7334 (2018).
 - ⁵⁹ Iain McKenzie, Masashi Harada, Robert F. Kiefl, C. D. Philip Levy, W. Andrew MacFarlane, Gerald D. Morris, Shin-Ichi Ogata, Matthew R. Pearson, and Jun Sugiyama, “ β -NMR measurements of lithium ion transport in thin films of pure and lithium-salt-doped poly(ethylene oxide),” *J. Am. Chem. Soc.* **136**, 7833–7836 (2014).
 - ⁶⁰ Iain McKenzie, David L. Cortie, Masashi Harada, Robert F. Kiefl, C. D. Philip Levy, W. Andrew MacFarlane, Ryan M. L. McFadden, Gerald D. Morris, Shin-Ichi Ogata, Matthew R. Pearson, and Jun Sugiyama, “ β -NMR measurements of molecular-scale lithium-ion dynamics in poly(ethylene oxide)-lithium-salt thin films,” *J. Chem. Phys.* **146**, 244903 (2017).
 - ⁶¹ Victoria L. Karner, Tianyi Liu, Iain Mckenzie, Aris Chatzichristos, David L. Cortie, Gerald D. Morris, Robert F. Kiefl, Ryan M. L. McFadden, Zahra Fakhraai, Monika Stachura, and W. Andrew Macfarlane, “Exploring the dynamics of glasses using beta detected NMR,” *JPS Conf. Proc.* **21**, 011022 (2018).
 - ⁶² Shingo Maruyama, Ida Bagus Hendra Prastiawan, Kaho Toyabe, Yuji Higuchi, Tomoyuki Koganezawa, Momoji Kubo, and Yuji Matsumoto, “Ionic conductivity in ionic liquid nano thin films,” *Acs. Nano.* **12**, 10509–10517 (2018).